arXiv:1609.06795v1 [cs.SY] 22 Sep 2016

An Internet of Lying Things: Probabilistic fault detection of nonverifiable sensors

Matthew A. Wright[1] and Roberto Horowitz[1]

***Abstract*— We are experiencing an explosion in the amount of sensors measuring our activities and the world around us. These sensors are spread throughout the built environment and can help us perform state estimation and control of related systems, but they are often built and/or maintained by third parties or system users. As a result, by outsourcing system measurement to third parties, the controller must accept their measurements without being able to directly verify the sensors' correct operation. Instead, detection and rejection of measurements from faulty sensors must be done with the raw data only. Towards this goal, we present a probabilistic formulation of state estimation with a model for possibly faulty behavior of sensors. We also take into consideration the possibility that the control designer may not know the characteristics of faulty measurements, and discuss how they may be alternatively detected by how much they differ from "expected" measurements. We detail implementation of the probabilistic formalism in a particle filtering application. Finally, we present results that use these methods, where the state of road traffic on a freeway is estimated via a particle filter by fusing third-party global navigational satellite system readings, while rejecting faulty measurements. The results demonstrate that faulty third-party measurements may be detected and removed without explicit models of a fault's characteristics.**

I. Introduction

Much ado has been made about the contemporary explosion of ubiquitous sensors and actuators in engineered artifacts and the built environment. "Big data," the "Internet of Things" - these and other recently-coined, oft-heard phrases call back to the idea that, in the past few years, a sea change has occurred in our ability to measure the world. For control and systems engineers, these new data increase the ability to measure and precisely control built-environment systems, with applications like localized responsive building HVAC regulation [1], connected vehicles for traffic management and accident reduction [2], and power systems, up to and including automated coordination between power producers, consumers, and storers in a "smart" grid [3]. When third-party measurements are collected and submitted by end users of Internet-of-Things devices and the like, fusion of these data can enhance the estimation and control of these sorts of highly-sensed and/or highly-actuated systems.

However, these new data can present their own problems. Whereas an engineer has traditionally designed control and estimation methods for a system whose components (including the sensors) she has been able to design and examine in detail, third-party data may be collected and submitted by a sensor that is faulty, overly noisy, tampered-with, or otherwise misreporting. It may not be feasible for the engineer to have a validated fault-detection method for every possible misconfiguration of every type of device that a third party might use to collect and report measurements.

In [4], for example, we considered a state estimator for road traffic that uses connected vehicles' speeds as reported by embedded global navigational satellite system (GNSS) transponders. An estimator might receive information that a vehicle had zero velocity on a road as indication that a traffic jam had formed and act accordingly. But if, instead, the vehicle was was stopped off the road but was misreporting its location due to GNSS drift, and no traffic jam was present, would the estimator be able to differentiate the two cases?

In this paper, we outline a simple method for rejection of potentially-faulty measurements such as these in the context of real-time state estimation. We previously used this method for the results presented in [4] but only briefly mentioned it there; the present paper contributes a detailed derivation and discussion. Section II gives a mathematical statement of our problem, and Section III gives a solution and discusses application details. We apply this solution to the widely-used particle filter algorithm, used for state estimation in nonlinear systems, in Section IV. The above stopped-car example is inspired by the work in [4] that in turn motivated the material presented in the present paper; Section V describes the application in [4]'s results, where faulty measurements from third-party GNSS devices were detected in a particle filtering application for estimating vehicle density on a freeway in southern California.

II. Problem Statement

Let $x_k \in \mathbb{R}^N$ denote the state vector of our system at time k, and $y_k \in \mathbb{R}^{M_k}$ denote the measurement vector at time k (note that y_k may be of different dimensionality at different times k). The state and observation vectors evolve over time through discrete-time stochastic state and output equations, denoted $\mathcal{F}_\theta(\cdot)$ and $\mathcal{G}_\theta(\cdot)$ respectively:

$$\begin{aligned} x_k &= \mathcal{F}_\theta\left(x_{k-1}\right) \\ y_k &= \mathcal{G}_\theta\left(x_k\right), \end{aligned} \tag{1}$$

with θ a parameter vector describing the randomness or process/measurement noise of $\mathcal{F}$ and $\mathcal{G}$. An alternative probabilistic notation may rewrite (1) as

$$X_k | \left(X_{k-1} = x_{k-1}\right) \sim f\left(x_k | x_{k-1}, \theta\right) \tag{2a}$$

$$Y_k | \left(X_k = x_k\right) \sim g\left(y_k | x_k, \theta\right), \tag{2b}$$

[1]Mechanical Engineering Department and Partners for Advanced Transportation Technologies, University of California, Berkeley, CA 94720, USA {mwright, horowitz}@berkeley.edu

where X_k (Y_k) denotes a random variable and x_k (y_k) the value of a particular realization. The functions $f(\cdot)$ and $g(\cdot)$ are the probability density functions (PDFs) induced by $\mathcal{F}_\theta(\cdot)$ and $\mathcal{G}_\theta(\cdot)$, respectively. The initial condition of the system, x_0, is assumed fixed or distributed with some known density $p(x_0|\theta)$. More precisely, $f(x_k|x_{k-1},\theta)$ is a Markov transition kernel with a distribution on the random variable $X_k|(X_{k-1}=x_{k-1})$, and $g(y_k|x_k,\theta)$ is a typical observation likelihood. To reduce notational clutter, we omit the symbol θ from now on.

In (2), the observation PDF is a joint PDF over all elements of the observation vector Y_k. This is the most general formulation of this PDF, and allows for all elements of Y_k to be statistically dependent. This would be appropriate, if, for example, the entire vector Y_k was reported by a single sensor, and the noise in measuring one element of Y_k was correlated with the noise in measuring the other elements.

In our setting, however, we are dealing with many different sensors and reporting devices. Say that Y_k contains measurements from m_k different sensors (like M_k (the length of Y_k), m_k may be different at different timesteps k), and let $k_j \in \{1,\dots,m_k\}$ index these sensors. Say that Y_{k_j} is the random vector that contains the element(s) of Y_k from sensor k_j. Now, if we assume that individual sensors k_j have statistically independent measurement noises, we may rewrite (2b) as (c.f. [4, Assumption 2, (14)])

$$Y_k|\left(X_k=x_k\right) \sim g\left(y_k|x_k\right) = \prod_{k_j=1}^{m_k} g_{k_j}\left(y_{k_j}|x_k\right), \tag{3}$$

where y_{k_j} is the measurement(s) received from sensor k_j (i.e., a realization of the random vector Y_{k_j}), and $g_{k_j}(\cdot)$ is the PDF for Y_{k_j}. We have factored $g(\cdot)$ into its component per-sensor PDFs.

As written in (3), $g_{k_j}(\cdot)$ is in a general form, with no explicit model of faulty vs non-faulty measurements. We now describe how we handle faulty sensors by explicitly indicating whether sensor k_j is reporting in either a valid (i.e., as intended) mode, or an erroneous mode. To this end, we introduce a Bernoulli random variable Z_{k_j}, which takes value 1 in the event that a measurement from sensor k_j is not faulty, and value 0 in the event that a measurement is faulty. Written as a probability mass function (PMF),

$$p(z_{k_j}|x_k) = \left(\phi_{k_j}(x_k)\right)^{z_{k_j}} \left(1-\phi_{k_j}(x_k)\right)^{\left(1-z_{k_j}\right)} \quad \text{for } z_{k_j}\in\{0,1\}, \tag{4}$$

where ϕ_{k_j} is a weight equal to the probability that sensor k_j reports a measurement in a valid, as-intended manner.

The parameter ϕ_{k_j} being a function of x_k allows for the possibility that the Z_{k_j} are dependent on X_k; that is, that certain areas of the state space for x_k could lead to a greater likelihood of erroneous measurements than others. This is the most general formulation, and we may simplify the problem by assuming independence of Z_{k_j} from X_k later.

Now, we can condition $g_{k_j}(\cdot)$ from (3) on Z_{k_j}:

$$g_{k_j}(y_{k_j}|z_{k_j},x_k) \triangleq g_{k_j}^{z_{k_j}}(y_{k_j}|x_k), \tag{5}$$

where $g_{k_j}^1(\cdot)$ is the PDF for the valid sensor behavior, and $g_{k_j}^0(\cdot)$ is the PDF for erroneous measurements. In practice, we should have a model for $g_{k_j}^1(\cdot)$, the expected behavior of the sensor, but $g_{k_j}^0(\cdot)$ may be unknown if we cannot predict every way in which the sensor may fail.

III. Fault detection

A. Solution

In this formulation, detecting a fault for a particular sensor k_j means determining whether z_{k_j} is equal to 0 or 1. Of course, z_{k_j} is not directly observable, and its value must be estimated alongside x_k from the observed y_{k_j}.

This can be written as a slight extension of traditional recursive Bayesian filtering. Let Z_k represent the collection of random variables Z_{k_j} at time k. Assume that at time k we have an estimate of the PDF $p(z_{k-1},x_{k-1}|y_{k-1})$. Then, we can predict Z_k and X_k before observing measurements Y_k:

$$\begin{aligned} p(z_k,x_k|y_{k-1}) =& p(z_k|x_k)\,p(x_k|y_{k-1}) \\ =& p(z_k|x_k)\Bigg(\sum_{z_{k-1}}\int p(z_{k-1},x_{k-1}|y_{k-1}) \\ & \times f(x_k|x_{k-1})dx_{k-1}\Bigg), \end{aligned} \tag{6}$$

and update our predictions once measurements Y_k have been received:

$$p(z_k,x_k|y_k) = \frac{p(z_k,x_k|y_{k-1})p(y_k|x_k,z_k)}{p(y_k|y_{k-1})}. \tag{7}$$

Equations (6) and (7) are the prediction and filtering steps, respectively, of recursive Bayesian filtering, with a slight modification in that Z_k is added. We will outline how these equations and PDFs are different from the standard formulation; a discussion of Bayesian filtering considering only the variables X_k and Y_k is available in many references.

Marginalization of the random variables Z_{k-1} and X_{k-1} in (6) is consistent with the marginalization of X_{k-1} in traditional Bayesian filtering; it relies on an assumption (explicit in the state space model (2)) that X_k and Z_k are conditionally independent of X_{k-1} and Z_{k-1} given Y_{k-1}.

The function $p(z_k|x_k)$ is the prior PMF of fault/non-fault sensor behavior (prior, in that it is the PMF of Z_k before the measurement vector Y_k is seen). The PDF $p(y_k|x_k,z_k)$ is the joint likelihood of this measurement vector Y_k from our unobserved system variables X_k and Z_k. Since, in (3), we assumed that the sensors k_j had independent measurement noises, and could factor the observation model across sensors k_j, we will do the same thing with these two functions:

$$p(z_k|x_k) = \prod_{k_j=1}^{m_k} p(z_{k_j}|x_k) \tag{8a}$$

$$p(y_k|x_k,z_k) = \prod_{k_j=1}^{m_k} g_{k_j}^{z_{k_j}}(y_{k_j}|x_k), \tag{8b}$$

with $p(z_{k_j}|x_k)$ and $g_{k_j}^{z_{k_j}}(y_{k_j}|x_k)$ from (4) and (5), respectively.

The marginal likelihood

$$p(y_k|y_{k-1}) = \sum_{z_{k-1}} \sum_{z_k} \iint p(z_{k-1}, x_{k-1}|y_{k-1}) f(x_k|x_{k-1}) \times p(z_k|x_k) p(y_k|x_k, z_k) dx_{k-1} dx_k \quad (9)$$

plays the role of a normalizing constant.

From the above equations, we can see that the determination of whether a sensor k_j is faulty at time k is done during the calculation of (7). If we focus on a particular sensor k_j, marginalizing out all other sensors in (7), the posterior PMF for Z_{k_j} for a particular value of X_k can be written as

$$\begin{aligned} p(z_{k_j}|x_k, y_{k_j}) &= \frac{p(z_{k_j}|x_k) p(y_{k_j}|x_k, z_{k_j})}{p(y_{k_j}|x_k)} \\ &= \frac{p(z_{k_j}|x_k) g_{k_j}^{z_{k_j}}(y_{k_j}|x_k)}{p(y_{k_j}|x_k)} \\ &= \frac{\left(\phi_{k_j}(x_k)\right)^{z_{k_j}} \left(1 - \phi_{k_j}(x_k)\right)^{(1-z_{k_j})} g_{k_j}^{z_{k_j}}(y_{k_j}|x_k)}{p(y_{k_j}|x_k)}. \quad (10) \\ &\text{for } z_{k_j} \in \{0, 1\}, \end{aligned}$$

From (10), we can see that determining the probability that a sensor is faulty is itself a Bayesian inference problem, with $p(z_{k_j}|x_k)$ being a prior distribution and $g_{k_j}^{z_{k_j}}(y_{k_j}|x_k)$ a likelihood. The denominator,

$$\begin{aligned} p(y_{k_j}|x_k) &= \sum_{z_{k_j}} p(z_{k_j}|x_k) p(y_{k_j}|x_k, z_{k_j}) \\ &= \sum_{z_{k_j}} p(z_{k_j}|x_k) g_{k_j}^{z_{k_j}}(y_{k_j}|x_k), \end{aligned} \quad (11)$$

again is a marginal likelihood that acts as a normalizing constant.

If we would like to compute $p(z_{k_j}|y_{k_j})$, averaging over all possible values of X_k, we can use the fact that Z_{k_j} is conditionally independent of Y_{k-1} given X_k to marginalize over X_k:

$$\begin{aligned} p(z_{k_j}|y_{k_j}) &= \int p(z_{k_j}|x_k, y_{k_j}, y_{k-1}) p(x_k|y_{k-1}) dx_k \\ &= \int p(z_{k_j}|x_k, y_{k_j}) p(x_k|y_{k-1}) dx_k. \end{aligned} \quad (12)$$

B. Empirical proportionality constants

Recall that we may only have a model of $g_{k_j}^{z_{k_j}}(y_{k_j}|x_k)$ for the case $Z_{k_j} = 1$, if we cannot predict every way a measurement might be faulty. In this case, the only value we can calculate from (10) is the numerator for the case that Z_{k_j} equals one, as computing (11) would require a model of $g_{k_j}^0(y_{k_j}|x_k)$. So from (10), dropping the normalizing denominator,

$$P(Z_{k_j} = 1|X_k = x_k, Y_{k_j} = y_{k_j}) \propto \phi_{k_j}(x_k) g_{k_j}^1(y_{k_j}|x_k), \quad (13)$$

and from (12),

$$\begin{aligned} P(Z_{k_j} = 1|Y_{k_j} = y_{k_j}) = & \int P(Z_{k_j} = 1|X_k = x_k, Y_{k_j} = y_{k_j}) \\ & \times p(x_k|y_{k-1}) dx_k \\ \propto & \int \phi_{k_j}(x_k) g_{k_j}^1(y_{k_j}|x_k) p(x_k|y_{k-1}) dx_k. \end{aligned} \quad (14)$$

Or, equivalently,

$$\begin{aligned} P(Z_{k_j} = 1|Y_{k_j} = y_{k_j}) = & \; C \int \phi_{k_j}(x_k) g_{k_j}^1(y_{k_j}|x_k) \\ & \times p(x_k|y_{k-1}) dx_k \end{aligned} \quad (15)$$

for some constant C.

We have replaced the normalizing denominators containing $g_{k_j}^0(\cdot)$ with a constant that must be estimated. While the constant C in (15) will almost certainly be different for every time k and sensor k_j, it makes sense to simplify the problem by having many sensors share the same value. This value could be estimated empirically through one of many methods. For example, it could be set such that the sensor with the highest value of the integral in (15) has a $P(Z_{k_j} = 1|Y_{k_j} = y_{k_j})$ equal to one, and other sensors are normalized against this best-performing sensor by using the same value of C. Or, if there is data available to calibrate model parameters against, one could perform several estimation runs over the state trajectory with varying values of C, and select a value that results in the best performance.

C. Fault probability thresholding

In practice, it is often desirable to be robust to faults, and to err on the side of caution when assimilating measurements that may be faulty. This is especially relevant if our models for $g_{k_j}^{z_{k_j}}(y_{k_j}|x_k)$ are estimates, and consequently cannot be certain that resulting estimates of $P(Z_{k_j} = 1|X_k = x_k, Y_{k_j} = y_{k_j})$ are accurate. In this case, it is reasonable to select some constant $\gamma \in (0, 1)$, and, for each sensor k_j, use (12) to determine whether $P(Z_{k_j} = 1|Y_{k_j} = y_{k_j}) > \gamma$. For sensors that do not meet this threshold and this inequality is false, we would use a fault probability of one when computing posterior PDFs, effectively discarding the sensor's measurement, and vice-versa for sensors where this inequality is true. For example, selecting $\gamma = 0.95$ means that we only assimilate measurements from sensors that we estimate have at least a 95% probability of being non-faulty.

D. Considerations for Application

We have two choices in how we may implement state estimation in this framework. First, we could perform the calculations of (6) and (7) and keep estimates of $p(z_k, x_k|y_k)$ for times k of interest, but this is hard to scale. If the size of an estimate of $p(x_k|y_k)$ is proportional to N (the dimensionality of X_k), the size of an estimate of the joint PDF $p(z_k, x_k|y_k)$ may be proportional to $N \cdot 2^{M_k}$ (recall M_k is the length of Y_k), since a different estimate of X_k may exist for every combination of faulty/not faulty of all sensor k_j. For all but trivial problems, this may be infeasible.

The second choice for implementation is to instead compute and store estimates of

$$p(x_k|y_k) = \sum_{z_k} p(z_k, x_k|y_k), \quad (16)$$

marginalizing out the variables Z_{k_j} and returning to our more manageable N-dimensional PDF. Since we are marginalizing along the z_{k_j}, the PDF $p(x_k|y_k)$ would be weighted by the estimated probability of fault of each sensor k_j.

E. Extension: Bayesian Updates of Fault Probabilities

It is usually the case that a particular sensor will report more than once, at different times k. In this case, it is reasonable to use past estimates of fault probability at times $k' < k$ to inform our prior fault probability ϕ_{k_j} at time k. A particularly simple method for this comes from Bayesian statistics: rather than letting $\phi_{k_j}(x_k)$ be fixed (that is, fixed for fixed values of x_k), we say that it is a random variable, and estimate it from Y_k as well. A Bernoulli random variable such as $\phi_{k_j}(\cdot)$ is often modeled as being drawn from a beta distribution, the conjugate prior of the Bernoulli distribution.

For a beta distribution for a particular sensor's fault probability, $\phi_{k_j} \sim \text{Beta}(\alpha_{k_j}, \beta_{k_j})$, we select the parameters based on prior belief about what values are more and less likely for ϕ_{k_j}. Then, when we wish to use a value for ϕ_{k_j} in, e.g., (4), some estimate of ϕ_{k_j}, such as a mean or modal value from its beta distribution, can be used instead. Finally, after we have obtained a posterior estimate of $Z_{k_j}|Y_{k_j}$, a Bayesian update of ϕ_{k_j}'s distribution is performed:

$$\begin{aligned}\phi_{k_j}|Y_{k_j} \sim \text{Beta}(&\alpha_{k_j} + P(Z_{k_j} = 1|Y_{k_j} = y_{k_j}),\\ &\beta_{k_j} + P(Z_{k_j} = 0|Y_{k_j} = y_{k_j}))\end{aligned} \tag{17}$$

and this new distribution is used as the prior when the sensor reports again at future times k.

IV. Particle Filter Implementation

The methods discussed so far make use of many PDFs (and integrals thereof). These operations may be performed in closed form when the PDFs can be expressed in closed form and the integrals are relatively simple, but this is often not the case when the system (1) is nonlinear.

For these situations, state estimation is often performed using Monte Carlo methods, with perhaps the most widely-used method being the particle filter [5]. A particle filter may be used when no closed-form model for $f(\cdot)$ exists (but the PDF may be sampled from by, e.g., running a stochastic simulation many times) and/or if numerically computing the integrals in (6) and (9) is computationally expensive.

A particle filter is constructed by replacing PDFs for X_k and Z_k with approximate PDFs made up of many discrete samples from the continuous PDF. We extend a traditional particle filter by including the random variable Z_k from (6):

$$\begin{aligned}p(z_k, x_k|y_{k-1}) &= p(z_k|x_k)\Bigg(\sum_{z_{k-1}}\int p(z_{k-1}, x_{k-1}|y_{k-1})\\ &\qquad\qquad \times f(x_k|x_{k-1})dx_{k-1}\Bigg)\\ &\approx\ p(z_k|x_k)\sum_{p=1}^{P}\Bigg(\sum_{z_{k-1}} p(z_{k-1}, x_{k-1}^p|y_{k-1})\delta_f(x_k^p|x_{k-1}^p)\Bigg)\\ &= p(z_k|x_k)\hat{p}(x_k|y_{k-1})\\ &= \hat{p}(z_k, x_k|y_{k-1}),\end{aligned} \tag{18}$$

where P is some integer denoting the total number of samples drawn from $f(\cdot)$, $p \in \{1, \ldots, P\}$ indexes individual samples (or atoms of the probability distribution), and $\delta_f\left(x_k^p|x_{k-1}^p\right)$ is the Dirac delta, which places a unit mass on the point $x_k^p|x_k^p$, itself denoting the value of the pth sample from $f(\cdot)$. The final two equalities indicate that the empirical PDF $\hat{p}(z_k, x_k|y_{k-1})$ consists of a weighted sum of P points $(z_k|x_k^p,\ x_k^p|x_{k-1}^p)$, with individual weights $p(x_k^p|y_{k-1})$, where the weights sum to one. A straightforward application of the strong law of large numbers shows that as $P \to \infty$, $\hat{p}\left(z_k, x_k|y_{k-1}\right) \to p\left(z_k, x_k|y_{k-1}\right)$ almost surely [5].

The corresponding particle filter update equation comes from plugging (18) into (7):

$$\begin{aligned}p(z_k, x_k|y_k) &= \frac{p(z_k, x_k|y_{k-1})p(y_k|x_k, z_k)}{p(y_k|y_{k-1})}\\ &\approx \frac{\hat{p}(z_k, x_k|y_{k-1})p(y_k|x_k, z_k)}{p(y_k|y_{k-1})}\\ &= \frac{1}{p(y_k|y_{k-1})}\Bigg(\sum_{p=1}^{P} p(z_k|x_k^p)p(y_k|x_k^p, z_k^p)\delta_f(x_k^p|x_{k-1}^p)\\ &\qquad\qquad \times \sum_{z_{k-1}} p(z_{k-1}, x_{k-1}^p|y_{k-1})\Bigg)\\ &= \frac{1}{p(y_k|y_{k-1})}\sum_{p=1}^{P} p(z_k^p, x_k^p|y_k)\delta_f(x_k^p|x_{k-1}^p)\\ &= \hat{p}(z_k, x_k|y_k).\end{aligned} \tag{19}$$

This posterior empirical PDF $\hat{p}(z_k, x_k|y_k)$ is thus made of the same collection of Dirac deltas as in $\hat{p}(z_k, x_k|y_{k-1})$, but with updated weights to reflect each point's updated probability (i.e., the prior probability times the likelihood).

Use of a particle filter also allows us to avoid having to calculate the marginal likelihood $p(y_k|y_{k-1})$ using (9) for use as a normalization constant in (19). Instead, after $p(z_k^p, x_k^p|y_k)$ is calculated for every particle p in (19), we normalize these probabilities such that they sum to one:

$$\hat{p}(z_k, x_k|y_k) = \sum_{p=1}^{P} \frac{p(z_k^p, x_k^p|y_k)\delta_f(x_k^p|x_{k-1}^p)}{\sum_{p=1}^{P} p(z_k^p, x_k^p|y_k)}. \tag{20}$$

In the particle filter framework, we can also perform a Monte Carlo approximation of $P(Z_{k_j} = 1|Y_{k_j} = y_{k_j})$ and related calculations from (10)-(14). Examining (14) in particular,

$$\begin{aligned}P(Z_{k_j}=1|Y_{k_j}=y_{k_j}) &= \int P(Z_{k_j}=1|X_k=x_k, Y_{k_j}=y_{k_j})\\ &\qquad \times p(x_k|y_{k-1})dx_k.\\ &= \int \frac{\phi_{k_j}(x_k)g_{k_j}^1(y_{k_j}|x_k)}{p(y_{k_j}|x_k)}p(x_k|y_{k-1})dx_k\\ &\approx \sum_{p=1}^{P} \frac{\phi_{k_j}(x_k^p)g_{k_j}^1(y_{k_j}|x_k^p)}{p(y_{k_j}|x_k^p)}\hat{p}(x_k^p|y_{k-1})\\ &= \hat{P}(Z_{k_j} = 1|Y_{k_j} = y_{k_j}).\end{aligned} \tag{21}$$

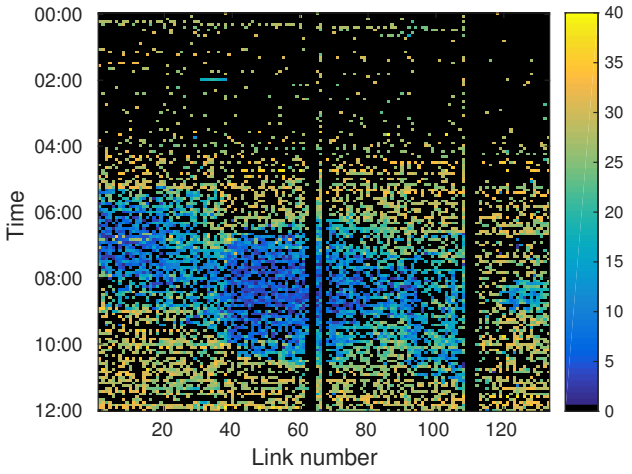

Fig. 1: GNSS speed (meters/second) readings from 2,613 individual sensors over twelve hours on Oct. 22, 2014. The raw lat-lon points are matched to links (discretized lengths of road) of roughly 300 meters. Black = no data.

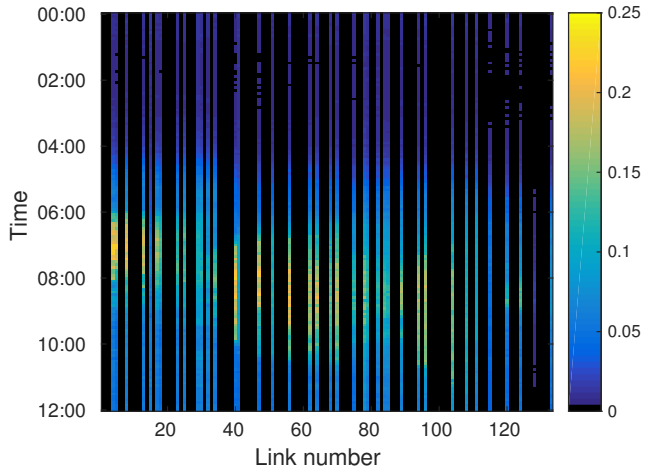

Fig. 2: Traffic density readings (vehicles/meter) from first-party inductive loop detectors. These density readings are converted from loop detectors' flow and speed measurements. They can be considered as more reliable than the GNSS measurements in Fig. 1. Black = no data.

All but one of the terms in (21) are always known: $\phi_{k_j}(x_k^p)$ and $g^1_{k_j}(y_{k_j}|x_k^p)$ can be computed for each particle p by plugging in the value of x_k^p into the relevant equations, and $\hat{p}(x_k^p|y_{k-1})$ is just the particle's prior probability from $\hat{p}(z_k, x_k|y_{k-1})$. The denominator, $p(y_{k_j}|x_k^p)$, again may be unsolvable if the form of $g^0_{k_j}(y_{k_j}|x_k)$ is not known, in which case the constant C from Section III-B is used.

An alternative fault detection scheme that might be more lenient would be to reject only measurements k_j that fail to pass some low threshold of non-fault probability for every particle:

$$P(Z_{k_j} = 1|X_k = x_k^p, Y_{k_j} = y_{k_j}) < \gamma \quad \forall p. \tag{22}$$

for small γ. This is alternative approximation of the integral the particle filter replaces. This might be appropriate if the engineer is concerned primarily with rejecting measurements that might cause numerical breakdown in the particle filter.

V. A CASE STUDY: GNSS SENSOR FUSION FOR HIGHWAY TRAFFIC STATE ESTIMATION

Recall our example of a traffic control system that took possibly faulty third-party data from connected vehicles' GNSS sensors to estimate the state of a road network. Accurate knowledge of traffic systems' operations is a key requirement for reactive traffic control, and gaining this knowledge from third-party data is a key part of modern intelligent transportation system applications.

In [4, Section IV-B], we presented results obtained using a particle filter that used the techniques detailed in Sections III and IV. We only briefly mentioned the use of the fault detection techniques in [4]; this section discusses them in detail. We estimated freeway traffic density using fused third- and first-party data. The particle filter used a finite-volume method known as the cell transmission model for its stochastic model $f(\cdot)$ (see [4] for full implementation details). We demonstrated the particle filter's performance on a 19-mile portion of I-210 West in southern California for the twelve-hour period from midnight to noon on October 22, 2014. For this period, we obtained measurements of vehicles' position and speed from GNSS devices near the area of interest (Fig. 1). We also obtained flow count data from inductive 35 loop detectors, which operate by passing an electric current through a buried metal loop and detect when a vehicle passes above and interferes with the magnetic field (Fig. 2). The loop detectors are installed and maintained by the California Department of Transportation [6], and their data can be considered first-party data and less prone to undetected faults than the third-party GNSS data.

A high vehicle density is predictive of congestion, and hence low vehicle speeds. While the time-space contour of the GNSS data shares many of the macro-scale features that appear in the loop data, it also has several features of low speed (i.e., high traffic density) that do not appear in the loop data. It is likely that these readings correspond to stopped cars adjacent to the highway whose lat-lon misidentified them as on the road, or outlier vehicles whose speed are not characteristic of the speed of traffic.

As an example, the string of low-speed points near 2:00 AM and link 40 (Fig. 1) are almost certainly faulty measurements, as they are not confirmed by high density in the loop data (Fig. 2) and high congestion in the early morning hours is not typical. A state estimation scheme that did not filter out these measurements would drive the state estimate to some unrealistic area of the state space.

In the results presented in [4], we performed fault detection and measurement rejection of the GNSS data to filter out measurements such as these. In particular, we used for the non-faulty GNSS measurement likelihood $g^1_{k_j}(y_{k_j}|x_k^p)$ a Gaussian distribution centered on the road link's velocity for the particle p and a variance equal to the sample variance for the link across all particles. The faulty GNSS model

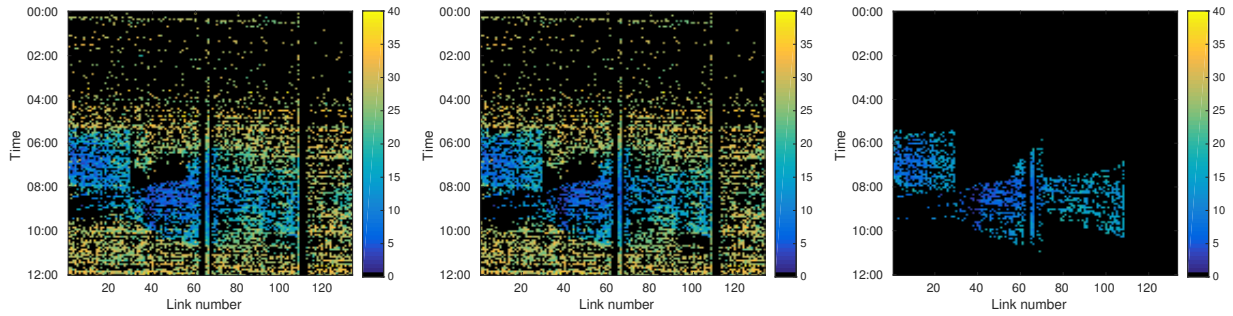

(a) $\gamma = 0.001$ (b) $\gamma = 0.01$ (c) $\gamma = 0.1$

Fig. 3: Subsets of GNSS velocity measurements (meters/second) in Fig. 1 that pass the probability threshold in (23) for various values of c. For $\gamma = 0.001$ (a), many points from Fig. 1 remain, but several isolated points with significantly different values than nearby surrounding points have been filtered out. Note that, while there are still a handful of points from the early-morning low-speed group discussed in Section V, the group's extent has been greatly reduced. For $\gamma = 0.01$ (b), these isolated early-morning points are completely removed, as well as several other groups. Note in particular that groups of points near the ending time period of congestion (e.g., near 9:00 and link 20) have been removed; one can see that these points were actually somewhat in disagreement with the inductive loop data (Fig. 2), which sees the congestion in this area mostly dispersing by 9:00. Finally, for $\gamma = 0.1$ (c), points have been filtered out through most of the area of the contour; only GNSS points that show high congestion concurrent with the loop detectors' high density observations remain.

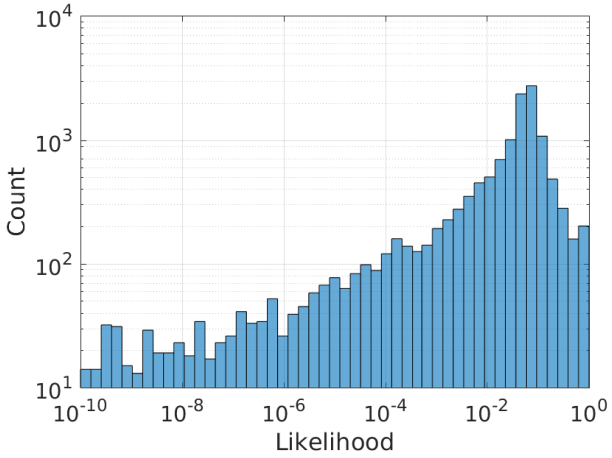

Fig. 4: Histogram of likelihood for GNSS velocity measurements from Fig. 1 (log scale). Points with likelihood below γ in (23) are excluded from the particle filter.

$g^0_{k_j}(y_{k_j}|x^p_k)$ was unknown, so following (22), sensors k_j where

$$P(Z_{k_j} = 1 | X_k = x^p_k, Y_{k_j} = y_{k_j}) \propto \phi_{k_j}(x^p_k) g^1_{k_j}(y_{k_j}|x^p_k) < \gamma \quad \forall p \qquad (23)$$

had their measurements rejected. In these results, a value of $\phi_{k_j}(x^p_k) = 0.5$ was used for all k_j and x^p_k.

High values of γ correspond to stricter rejection of faulty measurements - more sensors are caught in the inequality in (23) - while lower values are more forgiving (Fig. 3). In [4], a value of 0.01 for γ was used. This value was selected via hand-tuning. Automatic tuning of γ via iterated simulation, or in real-time in response to observed estimation error, would be a goal of future work. A histogram of empirical likelihoods for the GNSS measurements is given in Fig. 4.

VI. Conclusion

This paper considered a problem where state estimation is desired, but some measurements may be faulty in unknown ways. Our method for handling this problem explicitly weights measurements in the state estimator by their empirically-observed likelihood of known, correct-operational modes. While our method has a drawback in that, without a good model of faults, we must estimate a proportionality constant, this is unavoidable, as outsourcing sensing means that the controller cannot predict every way an outside sensor may malfunction.

Our discussion was in the context of sensors that are unintentionally faulty, but these methods are also applicable for robustness to falsified sensors. If a third party has control of sensors used by a control system, a malicious actor may feed spoofed measurements to the system to purposely manipulate its operation. Our fault-model-free method may complement existing defenses that actively search for patterns indicative of spoofed data: perhaps the lack of an explicit model for faulty or spoofed data may make it harder for attacks to be tailored to evade such a detector.

References

[1] J. Gubbi, R. Buyya, S. Marusic, and M. Palaniswami, "Internet of Things (IoT): A vision, architectural elements, and future directions," *Fut. Gen. Comp. Sys.*, vol. 29, no. 7, pp. 1645–1660, Sep. 2013.

[2] US DOT OTS-R, "ITS Research 2015-2019: Connected Vehicles," http://www.its.dot.gov/research_areas/connected_vehicle.htm, 2016.

[3] X. Fang, S. Misra, G. Xue, and D. Yang, "Smart Grid – The New and Improved Power Grid: A Survey," *IEEE Communications Surveys & Tutorials*, vol. 14, no. 4, pp. 944–980, 2012.

[4] M. Wright and R. Horowitz, "Fusing Loop and GPS Probe Measurements to Estimate Freeway Density," *IEEE Transactions on Intelligent Transportation Systems*, vol. PP, pp. 1–14, 2016.

[5] A. Doucet and A. M. Johansen, "A tutorial on particle filtering and smoothing: Fifteen years later," in *The Oxford Handbook of Nonlinear Filtering*. Oxford University Press, 2011, pp. 656–704.

[6] California Dept. of Tranportation, "PeMS," http://pems.dot.ca.gov.